Enhanced differentiation of functional human T cells in NSGW41 mice with tissue-specific expression of human interleukin-7.

Emilie Coppin[1,2*], Bala Sai Sundarasetty[3*§], Susann Rahmig[1,2], Jonas Blume[4], Nikita A. Verheyden[3], Franz Bahlmann[5], Sarina Ravens[4], Undine Schubert[9,10], Janine Schmid[9,10], Stefan Ludwig[11], Constantin von Kaisenberg[6], Alexander Platz[7], Ronald Naumann[8], Barbara Ludwig[9,10], Immo Prinz[4], Claudia Waskow[1,2,9,12$], Andreas Krueger[3$]

[1] Regeneration in Hematopoiesis, Institute for Immunology, TU Dresden, Dresden, Germany
[2] Immunology of Aging, Leibniz Institute on Aging - Fritz Lipmann Institute, Jena, Germany.
[3] Institute for Molecular Medicine, Goethe University Frankfurt am Main, Germany.
[4] Institute of Immunology, Hannover Medical School, Hannover, Germany.
[5] Department of Obstetrics and Gynecology, Bürgerhospital Frankfurt, Germany.
[6] Department Obstetrics, Gynecology and Reproductive Medicine, Hannover Medical School, Hannover, Germany.
[7] DKMS Cord Blood Bank, Dresden, Germany.
[8] Max-Planck Institute of Molecular Cell Biology and Genetics, Dresden, Germany.
[9] Department of Medicine III, Technical University Dresden, Dresden, Germany.
[10] German Center for Diabetes Research (DZD e.V.), Neuherberg, Germany.
[11] Department of Visceral-, Thorax- and Vascular Surgery, Technical University Dresden, Dresden, Germany.
[12] Institute of Biochemistry and Biophysics, Faculty of Biological Sciences, Friedrich-Schiller-University Jena, Jena, Germany.

* same contribution first authors

[$] joint supervision

[§] Current address: Recombinant Technologies, CSL Behring GmbH, Marburg, Germany

Corresponding author

Claudia Waskow

Claudia.waskow@leibniz-fli.de

Leibniz-Institute on Aging, Beutenbergstrasse 11, 07745 Jena, Germany

Phone: +49 3641 656 707

Key words: human IL-7, BAC, humanized mice, NSGW41, T cell, thymus, HSPC, cord blood, thymopoiesis, T cell activation

Key points

1. Increased intrathymic human T cell differentiation in the absence of pathological lymphoproliferation in humanized NSGW41hIL7 mice.

2. Increased peripheral human T cell populations in NSGW41hIL7 mice making the analysis of human regulatory T cells in vivo feasible.

Abstract

Humanized mouse models have become increasingly valuable tools to study human hematopoiesis and infectious diseases. However, human T cell differentiation remains inefficient. We generated mice expressing human interleukin (IL-7), a critical growth and survival factor for T cells, under the control of murine IL-7 regulatory elements. After transfer of human cord blood-derived hematopoietic stem and progenitor cells, transgenic mice on the NSGW41 background, termed NSGW41hIL7, showed elevated and prolonged human cellularity in the thymus while maintaining physiological ratios of thymocyte subsets. As a consequence, numbers of functional human T cells in the periphery were increased without evidence for pathological lymphoproliferation or aberrant expansion of effector or memory-like T cells. We conclude that the novel NSGW41hIL7 strain represents an optimized mouse model for humanization to better understand human T cell differentiation *in vivo* and to generate a human immune system with a better approximation of human lymphocyte ratios.

Introduction

Humanized mouse models have emerged as indispensable tools for improving our understanding of human hematopoiesis and the human immune system. Typically, they are generated by transplanting human hematopoietic stem and progenitor cells (HSPCs) into mice (for review see [1]). NSGW41 mice carry the hypomorph W41 allele in the *Kit* gene, harbor the NOD-specific variant of the *Sirpa* gene, are T-, B- and NK-cell deficient based on null mutations in *Prkdc* and *Il2rg* genes, and allow for human donor stem cell engraftment in the absence of preconditioning [2, 3]. NSGW41 mice that are stably engrafted with human hematopoietic stem cell display continuous human hematopoiesis with increased myeloid [2, 4], megakaryocytic and erythroid output compared to irradiated NSG recipient mice [5, 6].

The introduction of human genes to overcome selective deficiencies in human hematopoiesis has resulted in further improvement of humanized mouse models. Thus, mice expressing human cytokines, including a combination of SCF, GM-CSF, and IL-3 (NSG-SGM3) or M-CSF, IL-3, GM-CSF, and thrombopoietin (MISTRG) show improved myelopoiesis [7, 8]. Mice carrying a knock-in of human IL-6 show improved B-cell development and function [9].

Efficient differentiation of human T cells remains a challenge in humanized mice and we have focused on interleukin-7 (IL-7) to improve that situation. Patients with mutations in the *IL7RA* gene suffer from profound T–B+NK+ severe combined immunodeficiency [10]. In mice, loss of the *Il7ra* gene results in combined B and T-cell lymphopenia, pointing towards critical cross-species differences [11, 12]. *In vitro*, murine (m)IL-7 was 100-fold less potent to expand and differentiate human T-cell progenitors when compared to human (h)IL-7 [13]. Given its role as key factor for lymphocyte survival and proliferation [10-13], unrestricted supply of IL-7 might result in unwanted effects including lymphoma generation [14]. Further, excessive amounts of mIL-7 limits T cell differentiation by interfering with Notch signaling [15, 16]. Here, we generated hIL-7 (hIL-7) BAC transgenic NSGW41 mice to improve T cell differentiation in humanized mice while simultaneously avoiding unwanted effects caused by excessive and spatially unrestricted availability of hIL-7.

Results and Discussion

To generate a mouse model with tissue-specific expression of human (h)IL-7, we inserted cDNA encoding *IL7* into a BAC containing regulatory elements of the murine

100 *Il7* locus (Fig. 1a). BAC transgenic mice were generated on the NOD background,
101 crossed into the NSGW41 strain [2] and termed NSGW41hIL7. NSGW41hIL7 mice
102 contain three copies of the BAC transgene and expressed hIL-7 mRNA and protein in
103 BM, spleen and thymus (Fig. 1b,c). Engraftment of human HSPCs and T cell
104 differentiation was determined at indicated time points after transplantation of $CD34^+$-
105 enriched cord blood cells into unconditioned NSGW41 or NSGW41hIL7 mice (Fig.
106 1d). Blood from NSGW41 or NSGW41hIL7 mice contained comparable levels of
107 human hematopoietic cells peaking at 16-18 weeks after transplantation (Fig. 1e).
108 However, beginning at week 16 after transplantation frequencies of T cells among
109 human $CD45^+$ cells were significantly increased in NSGW41hIL7 mice compared to
110 NSGW41 recipients. Correspondingly, ratios of T and B cells increased progressively
111 over time, with T cells ultimately becoming the predominant lymphocyte population in
112 blood of NSGW41hIL7 mice (Fig. 1e,f). T/B ratios >1 are also observed in human
113 blood. Consistently, in spleens, human $CD45^+$ leukocytes were increased in
114 NSGW41hIL7 mice compared to NSGW41 mice, which was mainly attributable to
115 increased numbers of T cells (Fig. S1a,b). The data indicate that expression of hIL-7
116 under control of endogenous gene regulatory elements fosters T-cell differentiation in
117 NSGW41hIL7 mice.
118
119 Next, we assessed whether elevated frequencies of peripheral human T cells in
120 NSGW41hIL7 mice were due to more efficient intrathymic T-cell differentiation.
121 Human $CD45^+$ cell numbers were 3.3-fold, 3.5-fold, and 21.2-fold higher in thymi
122 from NSGW41hIL7 mice at 15, 18, and 26 weeks after reconstitution, respectively
123 (Fig. 2a). Ratios of human CD4/CD8 double negative (DN), double positive (DP), and
124 CD4 and CD8 single positive (SP) thymocytes were comparable in both recipient
125 lines 15 and 18 weeks after transplantation, indicating that ectopic expression of hIL-
126 7 did not result in aberrant T cell differentiation (Fig. 2b,c). NSGW41hIL7 but not
127 NSGW41 thymi predominantly contained DP thymocytes 26-32 weeks after
128 transplantation. In contrast, DN thymocytes constituted the major population in
129 NSGW41 mice, suggesting that hIL-7 supports human T cell differentiation for
130 extended periods of time in NSGW41hIL7 mice. A recently characterized combined
131 knock-in of hIL-7 and hIL-15 on the NSG background displayed massive skewing
132 towards CD8 SP cells at the expense of DP thymocytes [17], suggesting that tissue-
133 specific expression of human cytokines alone is insufficient to promote human T cell

134 differentiation [18]. Consistent with the T-lineage specific role of hIL-7 in human
135 hematopoiesis, and confirming specificity of transgenic expression of hIL-7, we
136 observed no alterations in B-cell differentiation in NSGW41hIL7 mice compared to
137 NSGW41 (Fig. 2d, S2a,b). We conclude that NSGW41hIL7 mice display improved
138 and extended intrathymic T cell differentiation from human cord blood-derived
139 HSPCs, temporally coinciding with a shift in T/B cell ratios in the periphery.
140
141 Elevated levels of human T-cell precursors in thymus suggested that the increased
142 frequencies of T cells in blood and spleen were largely reflecting increased thymic
143 output. However, hIL-7 might also alter peripheral homeostasis. To test this
144 possibility we further characterized peripheral T cell subsets in NSGW41hIL7 mice.
145 $CD4^+$ and $CD8^+$ T cell numbers in the blood were increased to comparable extent
146 (Fig. 3a). Within $CD4^+$ T cells, frequencies of naive T cells and Recent Thymic
147 Emigrants (RTEs) and effector T cells increased in NSGW41hIL7 mice compared to
148 NSGW41 (Fig. 3b,S3). Concomitantly, frequencies of effector memory T cells were
149 reduced. In $CD8^+$ T cells, a similar increase in naive and RTE and decrease in
150 effector memory frequencies was observed, whereas frequencies of T effector and
151 central memory subsets remained comparable to those detected in NSGW41 mice
152 (Fig. 3b, S3). Together, the relative contribution of different subsets to human T cells
153 in NSGW41hIL7 mice resembled the contribution in human peripheral blood. Next,
154 we analyzed T cell receptor (TCR) repertoire diversity using next-generation
155 sequencing to assess possible post-thymic peripheral expansion of T cells. This
156 analysis revealed a high frequency of rare T cell clones, which were comparable
157 between NSGW41 and NSGW41hIL7 mice. Virtually no expanded clones were
158 observed, indicating the absence of hIL-7-induced lymphoproliferation (Fig. 3c). We
159 conclude from these data that elevated peripheral frequencies of human T cells in
160 NSGW41hIL7 mice are largely generated through enhanced intrathymic T-cell
161 differentiation. Furthermore, this route of differentiation results in a composition of the
162 peripheral T-cell compartment largely resembling human peripheral blood. Paucity of
163 peripheral lymph nodes (LN), including mesenteric (m)LN, remains a critical limitation
164 of current NSG-derived humanized mouse models. In NSGW41hIL7 mice mLN were
165 increased in number and individual size compared to NSGW41 mice (Fig. 3d). Given
166 the poor regeneration of lymph nodes in other strains of humanized mice, this
167 observation suggests that NSGW41hIL7 mice might constitute an improved model for

168 studying gut-associated immune responses. Next, we characterized the functionality
169 of conventional human T cells in NSGW41hIL7 mice. To this end, we isolated and
170 activated *ex vivo* $CD3^+$ T cells from NSGW41 or NSGW41hIL7 spleens. Upregulation
171 of the bona fide activation markers CD25 and CD69 indicated similar levels of
172 activation (Fig. S4a). Finally, NSGW41hIL7-derived $CD4^+$ and $CD8^+$ T cells displayed
173 increased divisions in response to anti-CD3/CD28 or phytohemagglutinin stimulation
174 (Fig. 3e, S4). We conclude that human T cells differentiated in NSGW41hIL7 mice
175 respond efficiently to T cell receptor triggering *ex vivo*.
176
177 Regulatory T (Treg) cells are central in providing protection from autoreactive T cells
178 [19]. However, in the context of malignancy Treg-cell mediated immunosuppression
179 precludes effective anti-tumor immune responses [20]. Within the total T cell pool, Treg
180 cells constitute a comparatively small population, making their functional analysis
181 difficult in extant humanized mouse models with low overall T cell numbers. We
182 observed similar frequencies of regulatory T (Treg) cells in multiple organs from
183 NSGW41hIL7 or NSGW41 mice (Fig. 4a). However, given the higher overall T cell
184 numbers in NSGW41hIL7 mice, Treg cell numbers were increased making their
185 analysis feasible (Fig. 4a). To study the activation of Treg cells in humanized
186 NSGW41hIL7 mice, we transplanted porcine pancreatic islets into the portal vein of
187 humanized NSGW41hIL7 mice [4]. 18 hours after xenotransplantation, Treg cells in the
188 liver but not spleen displayed significantly increased expression of HLA-DR
189 evidencing site-specific activation through the xenograft (Fig. 4b). We conclude that
190 humanized NSGW41hIL7 mice represent a good model for the study of human Treg
191 cells *in vivo*.
192
193 Taken together, we have demonstrated that spatially restricted expression of hIL-7 in
194 NSGW41hIL7 mice results in an improved capacity for T-cell differentiation from
195 human HSPCs. Thus, we observed T/B cell ratios geared towards a higher
196 abundance of T cells when compared to NSGW41 and other humanized mouse
197 models [21]. Notably, increased intrathymic T-cell development promoted the
198 generation of a peripheral T-cell pool with a high TCR diversity and an overall
199 composition of T-cell subpopulations reminiscent of human peripheral blood.
200 Nevertheless, thymus size and cellularity in humanized NSGW41hIL7 mice remained
201 smaller than that of wild-type mice, suggesting that additional factors, presumably

202 depending on lymphocyte-stromal cell interactions, are required to generate a
203 normal-sized thymic microenvironment after humanization. It has been shown that
204 such a limitation can be partially overcome by co-transplantation of *in vitro*-
205 differentiated proT cells [22].
206 We detected no evidence for hIL-7-driven lymphoproliferation. We designed
207 NSGW41hIL7 mice to express hIL-7 using regulatory elements that allowed to
208 faithfully identify cells expressing mIL-7 in an earlier study [23]. Our study indicates that
209 this expression pattern and the observed levels of expression of hIL-7 are able to
210 strike a balance to overcome the limited potency of mIL-7 on human lymphocytes,
211 while at the same time avoiding detrimental effects of aberrant expression of hIL-7 [13,
212 14].
213 Enhanced T-cell differentiation in NSGW41hIL7 mice allowed for analysis of T cell
214 subsets, including Treg cells. In addition, size and number of mLN were increased.
215 Thus, humanized NSGW41hIL7 mice have the potential to foster investigation of rare
216 human T-populations in vivo as well as gut-associated immunity.
217
218 Methods
219 Generation of NSGW41hIL7 mice: NODhIL7 mice were generated by pronuclear
220 injection of a BAC containing codon-optimized cDNA of *hIL7* introduced at the 3' end
221 of the 5'UTR of the *Il7* gene flanked by 96kb upstream, and the entire *Il7* locus plus
222 an additional 17kb downstream. The BAC was constructed according to a described
223 strategy [23]. BAC integrity upon integration and copy numbers were determined by
224 PCR. Offspring showing detectable expression of hIL-7 mRNA was crossed with
225 NSGW41 mice [2] to generate the NSGW41hIL7 strain. All animal experiments were
226 performed in accordance with German animal welfare legislation and were approved
227 by the relevant authorities: Landesdirektion Dresden, the Thüringer Landesamt für
228 Verbraucherschutz, the Niedersächsisches Landesamt für Verbraucherschutz und
229 Lebensmittelsicherheit (LAVES), and the Regierungspräsidium Darmstadt.
230 Human HSPC transplantation: Cord blood samples were obtained from the
231 Department Obstetrics, Gynecology and Reproductive Medicine, Hannover Medical
232 School, Hannover, from the Bürgerhospital Frankfurt am Main, and from the DKMS
233 Cord Blood Bank, Dresden, and were used in accordance with the guidelines
234 approved by the ethics committees of Hannover Medical School, Frankfurt University
235 Clinics, Dresden University of Technology, and University Clinics Jena. $CD34^+$

236 HSPCs were isolated using dual magnetic beads enrichment according to the
237 manufacturer's instructions (Miltenyi Biotech) [2]. Purities >95% were considered
238 acceptable. Contaminating T cell frequencies were routinely below 1%.
239 Flow cytometry: Analysis was performed as described before [2]. A full list of antibody
240 panels is provided in Table S1.
241 TCR repertoire analysis: After mRNA isolation (Qiagen Micro Kit), cDNA was
242 generated via the Smarter 5'RACE cDNA amplification kit (Clontech) using 4.5µl
243 mRNA input and following the recommended protocol. Complementarity-determining
244 region 3 (CDR3) regions of the human TRB locus were amplified through a gene-
245 specific primer (2µM final concentration) that targets the constant region of the beta
246 (β)-chain (GCACACCAGTGTGGCCTTTTGGG) and a primer (1µM final
247 concentration) binding to the introduced SMARTER oligonucleotide
248 (CTAATACGACTCACTATAGGGC) using the Advantage 2 PCR kit (Clontech) in a
249 50µl reaction. Both primer sequences further contain 16S Illumina overhang adapter
250 sequences. Cycling conditions were as following: 120 s 95°C; 30 times 30 s 95°C, 45
251 s 64°C, 60 s 72°C; 60 s 72°C. Generated PCR amplicons were agarose gel purified
252 (Qiagen GelExtract.) Next, PCR samples were indexed with Nextera Illumina Indices
253 reads using the Advantage 2 PCR kit (Clontech) in a 8 PCR cycle reaction and
254 purified with Agencourt AMPpure XP beads (Beckman Coulter) according to the
255 manufacturers protocol. Samples were pooled, denatured and subjected to Illumina
256 MiSeq analysis using 500 cycles and paired-end sequencing following Illumina
257 guidelines. Sequencing libraries contained 20% PhIX for library complexity.
258 Demultiplexed Fastq files were annotated to the human TRB locus via MiXCR
259 software [18]. Individual CDR3 nucleotide sequences were ranked according to their
260 abundance within the respective samples and further analyzed using VDJTools [24]
261 and TcR [25]. TCR repertoire data are available at SRA
262 (https://www.ncbi.nlm.nih.gov/sra), accession number PRJNA606460.
263 Islet xenotransplantation: 500 IEQ (Islets Equivalent) adult pig islets or PBS were
264 transplanted in the portal vein of NSGW41hIL7 mice that were humanized 24 weeks
265 before. Islets were obtained from Goettingen minipigs (Ellgard) as described before
266 [26, 27]. Human blood cell chimerism of used mice was 32-85%. Regulatory T cells were
267 analyzed 18 hours after surgery.
268 T cell co-stimulation: $hCD3^+$ T cells were isolated from the spleen of humanized
269 NSGW41 or NSGW41hIL7 mice 16 to 25 weeks after HSPC transplantation,

270 enriched using negative depletion (Miltenyi), and CPD labeled (eBioscience). 10^5
271 $hCD3^+$ T cells were mixed with human T-Activator CD3/CD28 Dynabeads
272 (Thermofisher, ratio 3:1) or PHA (1µg/mL) in RPMI 10% FCS, 20mM L-glutamine,
273 10mM Hepes, 1mM Sodium Pyruvate, 50µM ß-mercaptoethanol with recombinant
274 hIL-2 (30 U/mL) and incubated for 6 days (37°C, 5% CO2).
275 Statistics: Student's t tests were performed for all statistical analyses using Prism 8
276 for MacOSX software. In all graphs *p = 0.05–0.01, **p = 0.01–0.001, and ***p =
277 0.001- 0.0001 and ****p < 0.0001; data represent the mean ± SD. Boxes and
278 whiskers display the data distribution through their quartiles.
279
280 References

281 1. Shultz, L.D. *et al.* Humanized mouse models of immunological diseases and
282 precision medicine. *Mammalian genome : official journal of the International*
283 *Mammalian Genome Society* 30, 123-142 (2019).
284 2. Cosgun, K.N. *et al.* Kit Regulates HSC Engraftment across the Human-Mouse
285 Species Barrier. *Cell Stem Cell* 15, 227-238 (2014).
286 3. Mende, N. *et al.* CCND1-CDK4-mediated cell cycle progression provides a
287 competitive advantage for human hematopoietic stem cells in vivo. *J Exp Med*
288 212, 1171-1183 (2015).
289 4. Rahmig, S., Bornstein, S.R., Chavakis, T., Jaeckel, E. & Waskow, C.
290 Humanized mouse models for type 1 diabetes including pancreatic islet
291 transplantation. *Hormone and metabolic research = Hormon- und*
292 *Stoffwechselforschung = Hormones et metabolisme* 47, 43-47 (2015).
293 5. Rahmig, S. *et al.* Improved human erythropoiesis and platelet formation in
294 humanized NSGW41 mice. *Stem Cell Reports* 7, 591-601 (2016).
295 6. Yurino, A. *et al.* Enhanced Reconstitution of Human Erythropoiesis and
296 Thrombopoiesis in an Immunodeficient Mouse Model with Kit(Wv) Mutations.
297 *Stem Cell Reports* 7, 425-438 (2016).
298 7. Nicolini, F.E., Cashman, J.D., Hogge, D.E., Humphries, R.K. & Eaves, C.J.
299 NOD/SCID mice engineered to express human IL-3, GM-CSF and Steel factor
300 constitutively mobilize engrafted human progenitors and compromise human
301 stem cell regeneration. *Leukemia* 18, 341-347 (2004).
302 8. Rongvaux, A. *et al.* Development and function of human innate immune cells
303 in a humanized mouse model. *Nat Biotechnol* 32, 364-372 (2014).

304 9. Yu, H. *et al.* A novel humanized mouse model with significant improvement of
305 class-switched, antigen-specific antibody production. *Blood* 129, 959-969
306 (2017).
307 10. Puel, A., Ziegler, S.F., Buckley, R.H. & Leonard, W.J. Defective IL7R
308 expression in T(-)B(+)NK(+) severe combined immunodeficiency. *Nat Genet*
309 20, 394-397 (1998).
310 11. Peschon, J.J. *et al.* Early lymphocyte expansion is severely impaired in
311 interleukin 7 receptor-deficient mice. *J Exp Med* 180, 1955-1960. (1994).
312 12. von Freeden-Jeffry, U. *et al.* Lymphopenia in interleukin (IL)-7 gene-deleted
313 mice identifies IL-7 as a nonredundant cytokine. *J Exp Med* 181, 1519-1526.
314 (1995).
315 13. van Lent, A.U. *et al.* IL-7 enhances thymic human T cell development in
316 "human immune system" Rag2-/-IL-2Rgammac-/- mice without affecting
317 peripheral T cell homeostasis. *J Immunol* 183, 7645-7655 (2009).
318 14. Rich, B.E., Campos-Torres, J., Tepper, R.I., Moreadith, R.W. & Leder, P.
319 Cutaneous lymphoproliferation and lymphomas in interleukin 7 transgenic
320 mice. *J Exp Med* 177, 305-316 (1993).
321 15. El-Kassar, N. *et al.* High levels of IL-7 cause dysregulation of thymocyte
322 development. *Int Immunol* 24, 661-671 (2012).
323 16. El Kassar, N. *et al.* A dose effect of IL-7 on thymocyte development. *Blood*
324 104, 1419-1427 (2004).
325 17. Matsuda, M. *et al.* Human NK cell development in hIL-7 and hIL-15 knockin
326 NOD/SCID/IL2rgKO mice. *Life science alliance* 2 (2019).
327 18. Bolotin, D.A. *et al.* MiXCR: software for comprehensive adaptive immunity
328 profiling. *Nat Methods* 12, 380-381 (2015).
329 19. Sakaguchi, S. *et al.* Regulatory T Cells and Human Disease. *Annu Rev*
330 *Immunol* (2020).
331 20. Yano, H., Andrews, L.P., Workman, C.J. & Vignali, D.A.A. Intratumoral
332 regulatory T cells: markers, subsets and their impact on anti-tumor immunity.
333 *Immunology* 157, 232-247 (2019).
334 21. Sippel, T.R., Radtke, S., Olsen, T.M., Kiem, H.P. & Rongvaux, A. Human
335 hematopoietic stem cell maintenance and myeloid cell development in next-
336 generation humanized mouse models. *Blood advances* 3, 268-274 (2019).

337 22. Awong, G. *et al.* Human proT-cells generated in vitro facilitate hematopoietic
338 stem cell-derived T-lymphopoiesis in vivo and restore thymic architecture.
339 *Blood* 122, 4210-4219 (2013).
340 23. Repass, J.F. *et al.* IL7-hCD25 and IL7-Cre BAC transgenic mouse lines: new
341 tools for analysis of IL-7 expressing cells. *Genesis* 47, 281-287 (2009).
342 24. Shugay, M. *et al.* VDJtools: Unifying Post-analysis of T Cell Receptor
343 Repertoires. *PLoS computational biology* 11, e1004503 (2015).
344 25. Nazarov, V.I. *et al.* tcR: an R package for T cell receptor repertoire advanced
345 data analysis. *BMC bioinformatics* 16, 175 (2015).
346 26. Ludwig, B. *et al.* Favorable outcome of experimental islet xenotransplantation
347 without immunosuppression in a nonhuman primate model of diabetes. *Proc*
348 *Natl Acad Sci U S A* 114, 11745-11750 (2017).
349 27. Steffen, A. *et al.* Production of high-quality islets from goettingen minipigs:
350 Choice of organ preservation solution, donor pool, and optimal cold ischemia
351 time. *Xenotransplantation* 24 (2017).
352
353
354 Acknowledgements
355 We are grateful to Katrin Witzlau and Esther Imelmann for technical assistance and
356 management of mouse colonies. We would like to thank Dr. Ellen Richie (MD
357 Anderson Cancer Center, TX, USA) for providing BAC constructs and advice on
358 cloning. The work was supported by grants from the German Research Foundation
359 (DFG, SFB738-A7 and SFB902-B15) (to A.K.) and FOR2033-A03, TRR127-A5,
360 WA2837/6-1 and WA2837/7-1 (to C.W.).
361
362 Authorship contributions
363 E.C. planned, conducted, interpreted experiments and wrote the paper. B.S. planned,
364 conducted and interpreted experiments. S.Rah, J.B., and N.V. conducted
365 experiments. J.B., S.Rav., and I.P. conducted and interpreted experiments on TCR
366 repertoire. U.S., J.S., S.L. and B.L. isolated and provided porcine islets for
367 xenotransplanation. F.B., C.v.K, and A.P. provided crucial reagents. R.N. generated
368 knock-in mice, and C.W. and A.K. conceived the study, planned and interpreted
369 experiments and wrote the paper.
370

371 Disclosure of conflicts of interest

372 The authors declare that no conflicts of interest exist.

373

374 Figure legends

375 **Fig. 1: Enhanced generation of human T cells upon transfer of human HSPCs**
376 **in NSGW41hIL7 mice. a**, Scheme of BAC construct for the generation of
377 NSGW41hIL7 mice. **b**, Abundance of hIL7 transcript in bone marrow (BM), spleen
378 and thymus from humanized NSGW41 or NSGW41hIL7 mice. Each dot represents
379 an individual mouse. **c**, hIL7 protein levels in thymi isolated from non-humanized
380 NSGW41 or NSGW41hIL7 mice (top) and in bone marrow, thymus and serum from
381 NSGW41 or NSGW41hIL7 mice that have received human HPSCs 26-38 weeks
382 before (bottom). **d**, Scheme of transplantation experiments. **e**, Kinetics of the
383 appearance of human $CD45^+$ cells ($hCD45^+$, left) and $hCD3^+$ T cells within human
384 leukocytes (right) in the blood after humanization. Each dot represents an individual
385 mouse. **f**, Frequencies of T cells, B cells and non-defined other cells of human origin
386 in the blood of NSGW41 (n=13) or NSGW41hIL7 (n=16) mice 18 weeks after
387 humanization. Numbers on top indicate T vs. B cell ratios.

388

389 **Fig. 2: Efficient and prolonged intrathymic T-cell differentiation in humanized**
390 **NSGW41hIL7 mice. a**, Numbers (top) and fold-change (bottom) of human $CD45^+$
391 cells in thymi of humanized NSGW41 or NSGW41hIL7 mice at the indicated time
392 points after humanization. Fold-changes were calculated by dividing human $CD45^+$
393 thymocyte numbers from humanized NSGW41hIL7 mice through the thymocyte
394 numbers from humanized NSGW41 mice. This was done separately for each
395 experiment and the results pooled. **b**, Analysis of CD4 and CD8 expression on
396 $hCD45^+$ thymocytes from NSGW41 or NSGW41hIL7 mice that have received human
397 HPSCs 15 weeks (left) or 26 (right) weeks before. **c**, Distribution of thymocyte
398 subsets in NSGW41 or NSGW41hIL7 mice at the indicated time points after
399 humanization. **d**, Numbers of B cells subsets in the bone marrow of NSGW41 or
400 NSGW41hIL7 mice 26 weeks after humanization.

401

402 **Fig. 3: hIL7-BAC transgene increases functional peripheral T cells in the**
403 **absence of excessive lymphoproliferation. a**, Human $CD4^+$ and $CD8^+$ T cells in
404 the blood of humanized NSGW41 or NSGW41hIL7 mice 26 weeks after

405 humanization. **b**, Composition of blood $CD4^+$ (top) and $CD8^+$ (bottom) T cell
406 subpopulations 26 weeks after humanization: Naïve T cells, central memory (T_{CM}),
407 effector memory (T_{EM}), T effector (T_{EFF}) and recent thymic emigrants (RTE) in
408 NSGW41, NSGW41hIL7 mice, or human blood. **c**, T cell receptor (TCR) repertoire
409 diversity in splenic αβ T cells of NSGW41 or NSGW41hIL7 mice. Clones were binned
410 into rare ($0<X\leq0.001$), small ($0.001<X\leq0.01$), medium ($0.01<X\leq0.1$) and expanded
411 ($0.1<X\leq1$) (n=3 per group). **d**, Photographs of mLN from humanized NSGW41 or
412 NSGW41hIL7 mice isolated 26 weeks after humanization, or C57BL/6 controls (top).
413 mLN number per mouse (bottom left). $hCD45^+$ and $hCD3^+$ cell numbers in mLN from
414 NSGW41 or NSGW41hIL7 mice isolated 26 weeks after humanization (bottom right).
415 **e**, Activation of human T cells from NSGW41 or NSGW41hIL7 mice. Histograms
416 depict division of CDP-labeled spleen $hCD3^+$ T cells 6 days after stimulation with
417 CD3/28 beads or control (w/o, left). Frequencies of non-divided human T cells and T
418 cells that have divided 4, 5 or 6 times 6 days after stimulation with CD3/28 antibody-
419 coated beads or controls (right). Top: $CD4^+$ T cells, bottom: $CD8^+$ T cells.
420
421 **Fig. 4: Efficient generation of human Treg cells in NSGW41hIL7 mice. a**,
422 Representative dot plots analyzing mesenteric lymph nodes (mLN) and blood (left)
423 and numbers (right, top) and frequencies (right, bottom) of Tregs in mLN, blood,
424 spleen and liver of humanized NSGW41 or NSGW41hIL7 mice. **b**, Human activated
425 Tregs after intraportal xenotransplantation of porcine pancreatic islets into
426 NSGW41hIL7 mice 26 weeks after humanization. Representative dot plots of liver
427 and spleen analysis (left). Frequencies of $HLA\text{-}DR^+$ $FoxP3^+$ T cells in spleen and liver
428 of humanized NSGW41hIL7 mice (right) 18 hours after transplantation of islets (iTx)
429 or PBS.
430

Figure 1

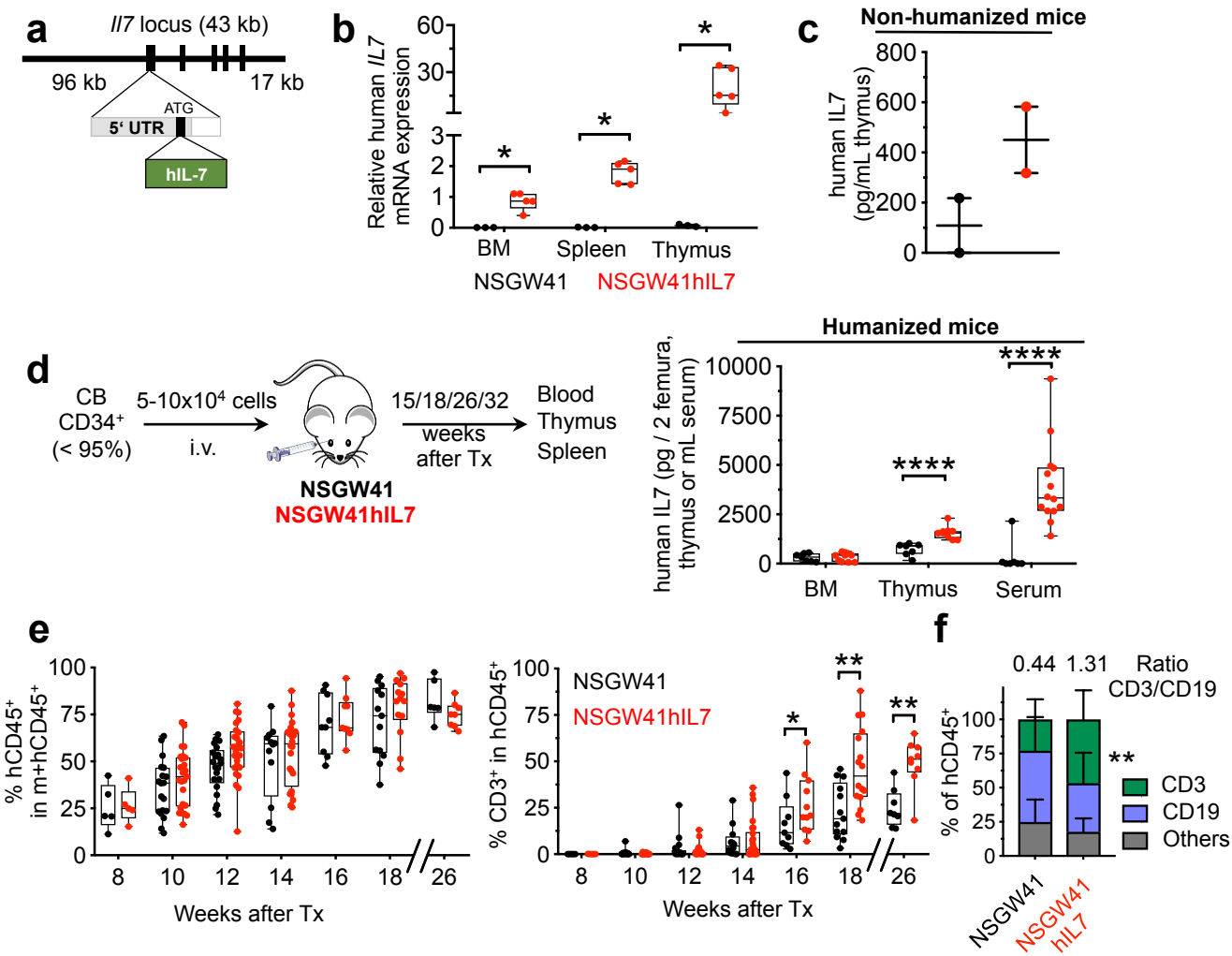
a
Il7 locus (43 kb)
96 kb
17 kb
ATG
5' UTR
hIL-7
b
Relative human IL7 mRNA expression
BM
Spleen
Thymus
NSGW41
NSGW41hIL7
c
Non-humanized mice
human IL7 (pg/mL thymus)
d
CB CD34+ (< 95%)
5-10x10^4 cells
i.v.
15/18/26/32 weeks after Tx
Blood
Thymus
Spleen
NSGW41
NSGW41hIL7
Humanized mice
human IL7 (pg / 2 femura, thymus or mL serum)
BM
Thymus
Serum
e
% hCD45+ in m+hCD45+
Weeks after Tx
% CD3+ in hCD45+
NSGW41
NSGW41hIL7
f
0.44 1.31 Ratio CD3/CD19
% of hCD45+
CD3
CD19
Others
NSGW41
NSGW41 hIL7

Figure 2

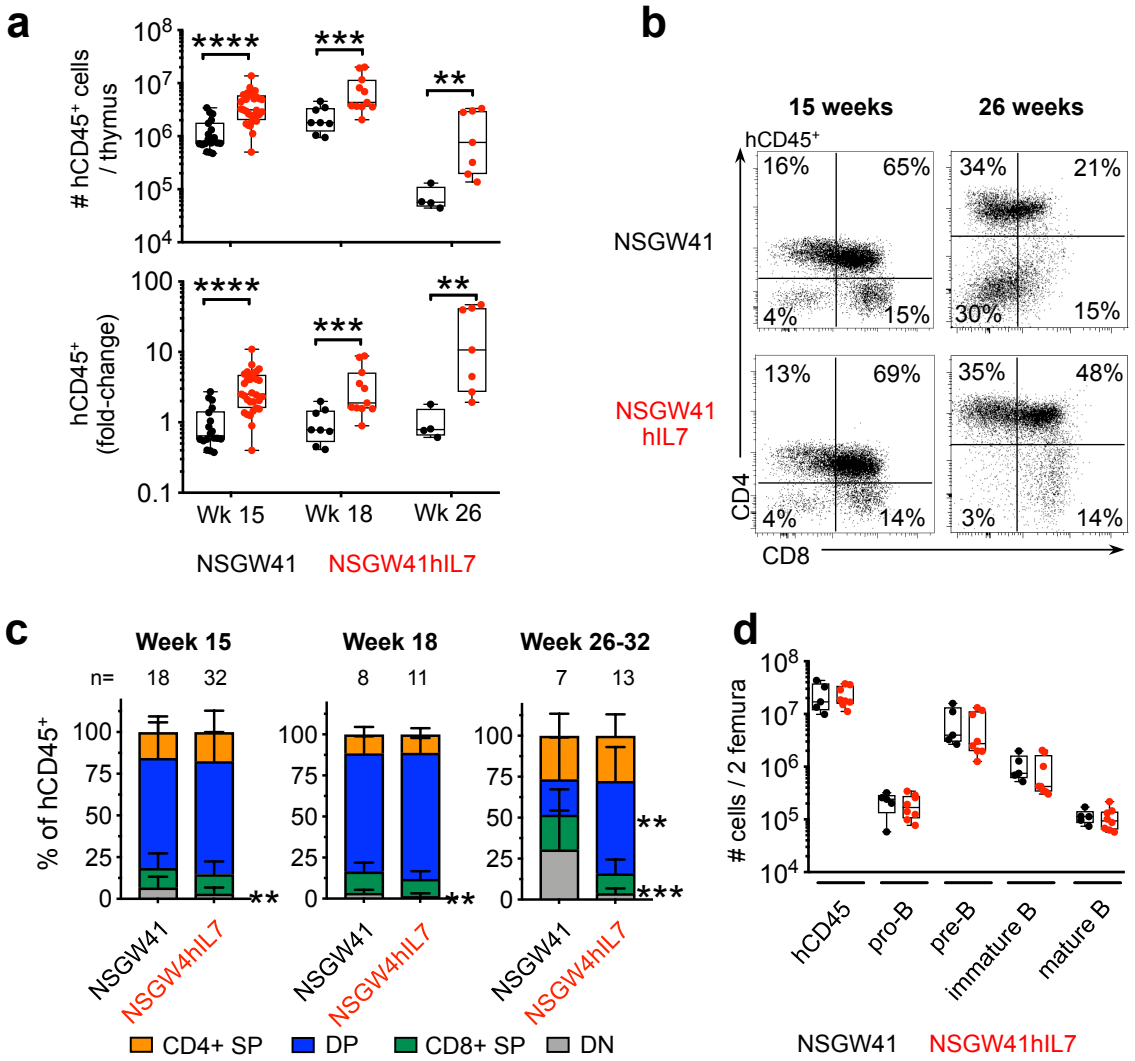
a
hCD45+ cells / thymus
hCD45+ (fold-change)
Wk 15
Wk 18
Wk 26
NSGW41
NSGW41hIL7
b
15 weeks
26 weeks
hCD45+
NSGW41
NSGW41 hIL7
CD4
CD8
16%
65%
4%
15%
34%
21%
30%
15%
13%
69%
4%
14%
35%
48%
3%
14%
c
Week 15
Week 18
Week 26-32
n=
18
32
8
11
7
13
% of hCD45+
NSGW41
NSGW4hIL7
CD4+ SP
DP
CD8+ SP
DN
d
cells / 2 femura
hCD45
pro-B
pre-B
immature B
mature B
NSGW41
NSGW41hIL7

Figure 3

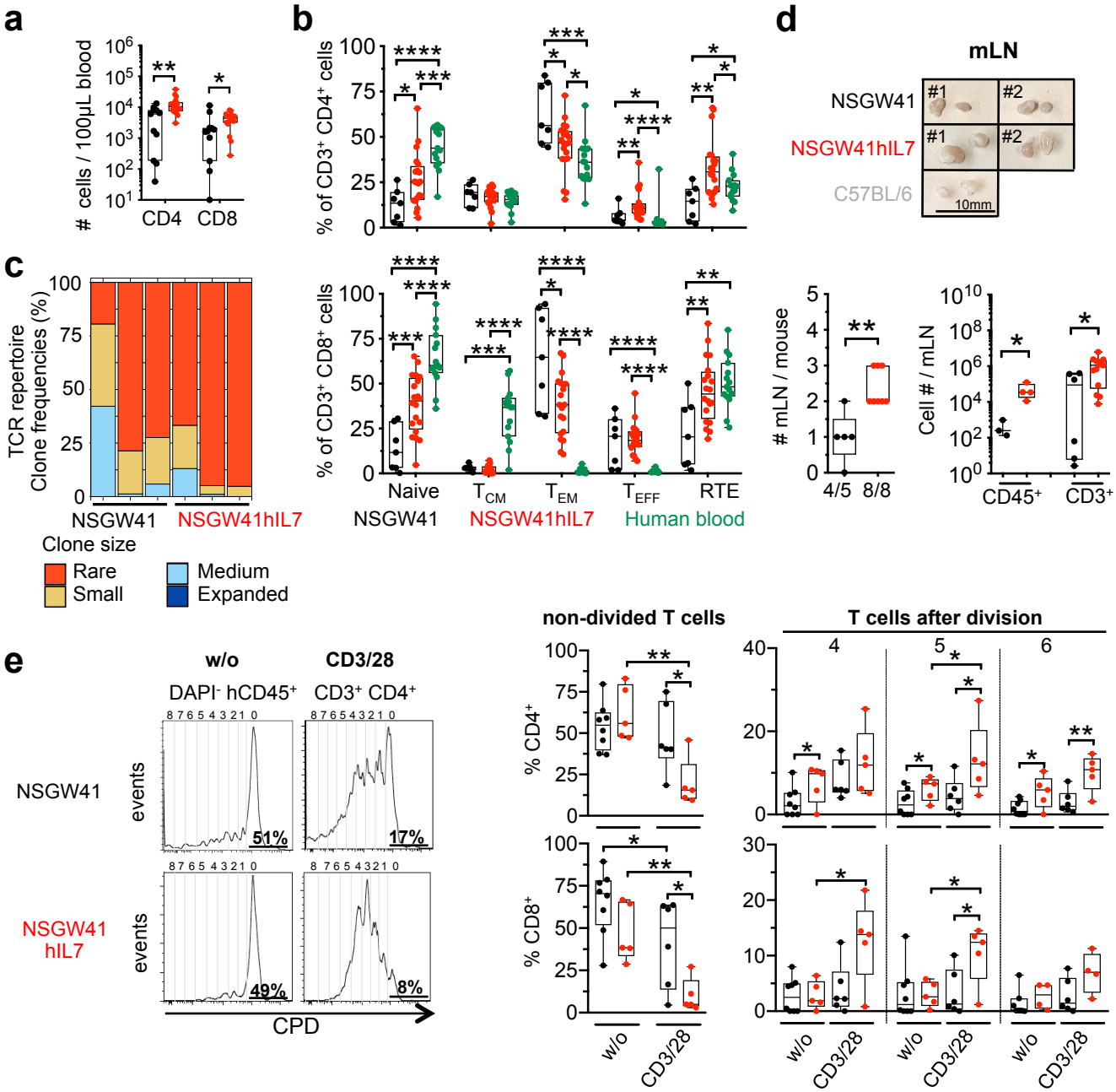
a
cells / 100µL blood
CD4
CD8
b
% of CD3+ CD4+ cells
% of CD3+ CD8+ cells
Naive
TCM
TEM
TEFF
RTE
NSGW41
NSGW41hIL7
Human blood
c
TCR repertoire
Clone frequencies (%)
NSGW41
NSGW41hIL7
Clone size
Rare
Small
Medium
Expanded
d
mLN
NSGW41
NSGW41hIL7
C57BL/6
#1
#2
10mm
mLN / mouse
4/5
8/8
Cell # / mLN
CD45+
CD3+
e
w/o
CD3/28
DAPI- hCD45+
CD3+ CD4+
events
51%
17%
49%
8%
CPD
non-divided T cells
T cells after division
% CD4+
% CD8+
w/o
CD3/28

Figure 4

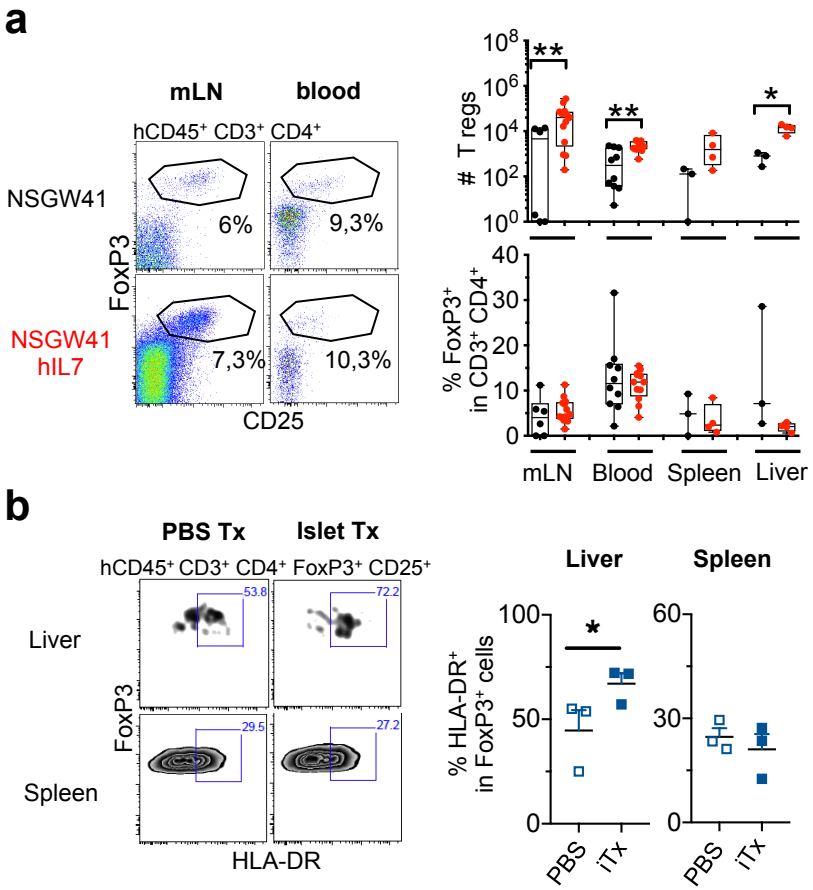
a
mLN
blood
hCD45+ CD3+ CD4+
NSGW41
NSGW41
hIL7
6%
9,3%
7,3%
10,3%
FoxP3
CD25
T regs
% FoxP3+ in CD3+ CD4+
mLN
Blood
Spleen
Liver
b
PBS Tx
Islet Tx
hCD45+ CD3+ CD4+ FoxP3+ CD25+
Liver
Spleen
53.8
72.2
29.5
27.2
FoxP3
HLA-DR
Liver
Spleen
% HLA-DR+ in FoxP3+ cells
PBS
iTx
PBS
iTx

Supplemental Material

Enhanced differentiation of functional human T cells in NSGW41 mice with tissue-specific expression of human interleukin-7.

Emilie Coppin[1,2*], Bala Sai Sundarasetty[3*§], Susann Rahmig[1,2], Jonas Blume[4], Nikita A. Verheyden[3], Franz Bahlmann[5], Sarina Ravens[4], Undine Schubert[9,10], Janine Schmid[9,10], Stefan Ludwig[11], Constantin von Kaisenberg[6], Alexander Platz[7], Ronald Naumann[8], Barbara Ludwig[9,10], Immo Prinz[4], Claudia Waskow[1,2,9,12$], Andreas Krueger[3$]

12 Table S1

13

Antibodies	Clone	Provider
CD3 APC, AF780, APC Cy7	UCHT1, HIT3a	eBioscience
CD4 PE Cy7, Pacific Blue	OKT-4/RPA-T4	eBioscience
CD8 PE Cy5, PerCP, PE Cy7	SK1, HIT8a	eBioscience
CD10 APC Cy7	HI10a	BioLegend
CD14 AF700	M5E2	BD Pharmingen
CD16 PerCP, PE Cy5	3G8	BioLegend, BD Biosciences
CD19 FITC, PC7, APC, FITC	HIB19	eBioscience
CD25 PE	M-A251	BioLegend, BD Biosciences
CD31 PE	MEM-05	Immunotools
CD33 PE, PE Cy7	WM-53	eBioscience
CD34 PE Cy7, Pacific Blue	OKT-4/RPA-T4	eBioscience
mCD45 AF780, AF700	RA3-6B2	eBioscience
hCD45 eF450, FITC, PE Cy7, PerCP	HI30	eBioscience, BioLegend
CD45RA eF450	HI100	eBioscience
CD45RO FITC, PE	UCHL1	BD Biosciences
CD62L Biotin	DREG.55	eBioscience
CD69 PerCP Cy5.5	Y1/82A	BioLegend
CD197 APC, BV510	REA337, G043H7	Miltenyi
CD235 FITC	GA-R2 (HIR2)	eBioscience
Foxp3 APC	PCH101	eBioscience
HLA DR PerCP Cy5.5	4S.B3	BioLegend
IgD PE	IA6-2	BD Pharmingen
IgM Biotin	SA-DA4	BioLegend
Ter119 FITC	11-5921-82	eBioscience
Streptavidin V500, FITC	na	BD Biosciences, BD Pharmingen
Cell Proliferation Dye eF450	na	ebioscience
Fixabe viability dye AF700	na	BD Biosciences

14

15

16 **Supplementary figures**

17

18

19

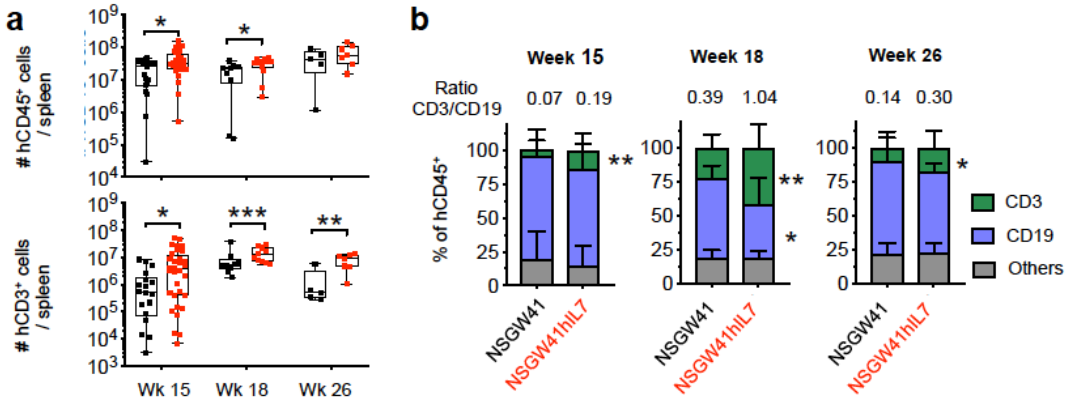

20

21

22 **Supplementary Figure 1: Human lymphocyte composition in spleen.** (**a**)
23 Numbers of hCD45$^+$ leukocytes (top) and hCD3$^+$ T cells (bottom) in spleens of
24 NSGW41 or NSGW41hIL7 mice 15, 18 and 26 weeks after humanization. (**b**)
25 Frequencies of hCD3$^+$, hCD19$^+$, and other cells within hCD45$^+$ leukocytes in spleens
26 of NSGW41 or NSGW41hIL7 mice 15, 18 and 26 weeks after humanization.
27 Numbers on top of graphs indicate T vs. B cell ratio.

28

29

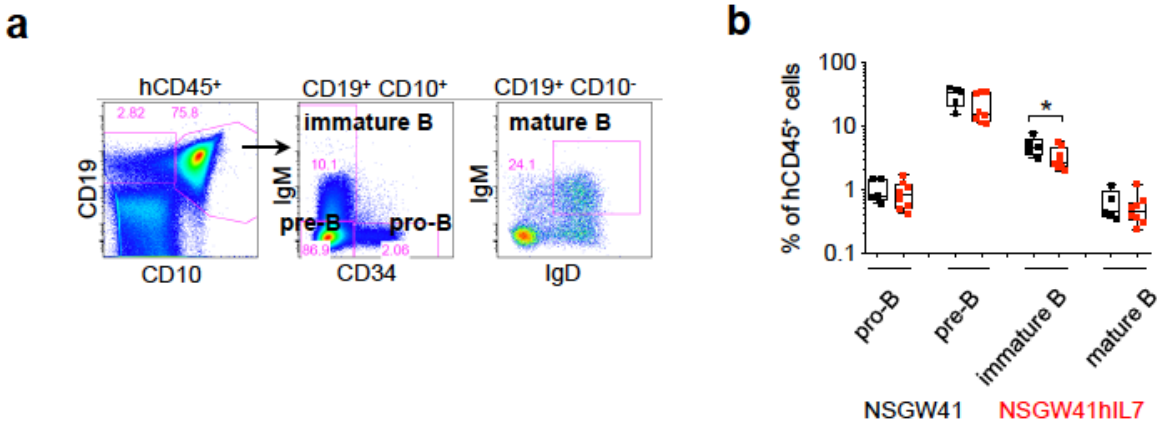

30

31 **Supplementary Figure 2: B lymphopoiesis in NSGW41hIL7 mice.** (**a**) Dot plots
32 show the gating strategy of bone marrow human B lineage subsets: pro-B (hCD45^{+}
33 CD19^{+} CD10^{+} IgM^{-} CD34^{+}), pre-B (hCD45^{+} CD19^{+} CD10^{+} IgM^{-} CD34^{-}), immature B
34 (hCD45^{+} CD19^{+} CD10^{+} IgM^{+} CD34^{-}) and mature B cells (hCD45^{+} CD19^{+} CD10^{-} IgM^{+}
35 IgD^{+}). (**b**) Frequencies of B cell subsets in bone marrow of humanized mice 26
36 weeks after humanization.

37

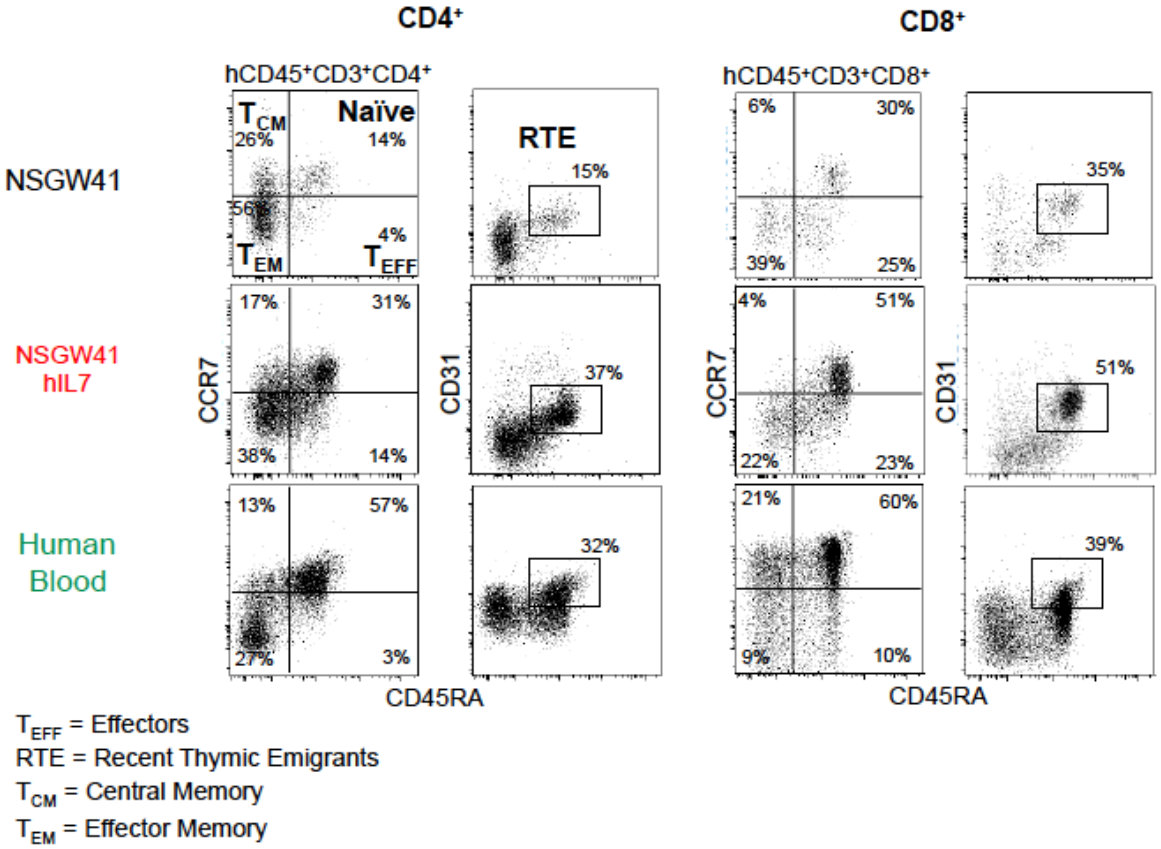

38

39 **Supplementary Figure 3: Characterization of human T cell subpopulations in**
40 **the blood.** Gating strategy and identification of hCD4$^+$ and hCD8$^+$ T cell
41 subpopulations in blood of humanized mice: T effectors (T_{EFF}, hCD45$^+$ CD3$^+$ CD4$^+$
42 CCR7$^-$ CD45RA$^+$), central memory (T_{CM}, hCD45$^+$ CD3$^+$ CD4$^+$ CCR7$^+$ CD45RA$^-$),
43 effector memory (T_{EM}, hCD45$^+$ CD3$^+$ CD4$^+$ CCR7$^-$ CD45RA$^-$), naïve T (Naïve, hCD45$^+$
44 CD3$^+$ CD4$^+$ CCR7$^+$ CD45RA$^+$) and recent thymic emigrants (RTE, hCD45$^+$ CD3$^+$ CD4$^+$
45 CD31$^+$ CD45RA$^+$). Data was acquired 26 weeks after humanization. The composition
46 of subpopulations in human blood is shown for comparison (bottom).

47

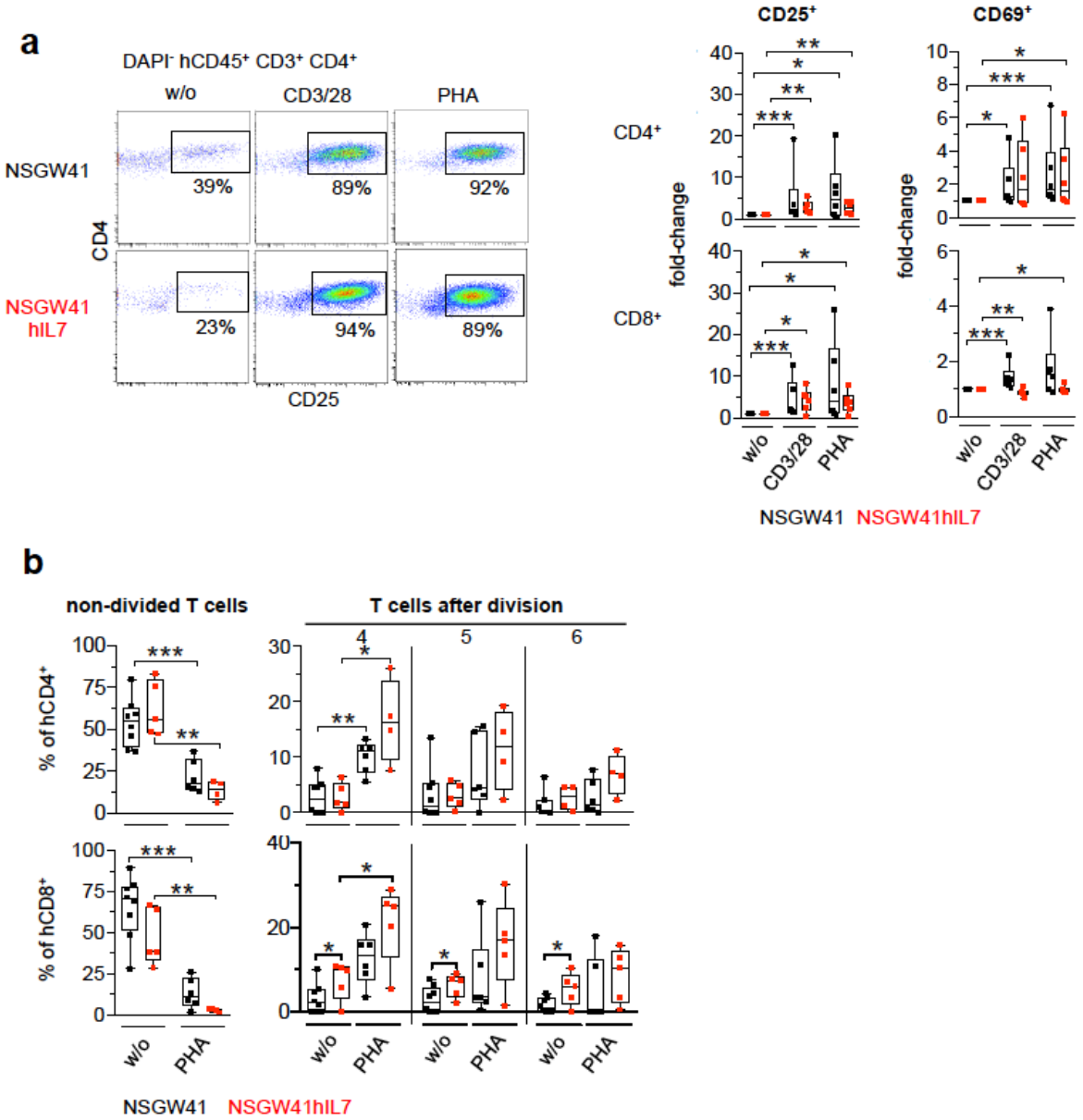

48

49 **Supplementary Figure 4: Activation of human T cells from NSGW41 or**
50 **NSW41hIL7 mice.** (**a**) Representative dot plots showing the expression of hCD25
51 and hCD69 on hCD3$^+$ T cells isolated from NSGW41 (top) or NSGW41hIL7 (bottom)
52 spleens after 6 days of CD3/28 or PHA stimulation or non-stimulated controls (left).
53 Donor mice had received human HSPCs 20 to 26 weeks before. Fold-changes were
54 calculated by dividing the percentages of stimulated hCD25$^+$ or hCD69$^+$ hCD4$^+$ (top)
55 or hCD8$^+$ (bottom) splenic T cells by the percentages of non-stimulated cells (w/o)
56 from NSGW41 or NSGW41hIL7 mice (right). (**b**) Percentages of non-divided T cells
57 and T cells which have undergone 4, 5 or 6 divisions 6 days after stimulation with
58 phytohemagglutinin (PHA) or without stimulation (w/o). Top: hCD4$^+$ T cells, bottom:
59 hCD8$^+$ T cells. Donor mice had received human HSPCs 20 to 26 weeks before.